World Academy of Science, Engineering and Technology
International Journal of Mechanical and Mechatronics Engineering
Vol:8, No:7, 2014

Dynamic Behavior of Brain Tissue under Transient Loading

Y. J. Zhou, G. Lu

***Abstract*—**In this paper, an analytical study is made for the dynamic behavior of human brain tissue under transient loading. In this analytical model the Mooney-Rivlin constitutive law is coupled with visco-elastic constitutive equations to take into account both the nonlinear and time-dependent mechanical behavior of brain tissue. Five ordinary differential equations representing the relationships of five main parameters (radial stress, circumferential stress, radial strain, circumferential strain, and particle velocity) are obtained by using the characteristic method to transform five partial differential equations (two continuity equations, one motion equation, and two constitutive equations). Analytical expressions of the attenuation properties for spherical wave in brain tissue are analytically derived. Numerical results are obtained based on the five ordinary differential equations. The mechanical responses (particle velocity and stress) of brain are compared at different radii including 5, 6, 10, 15 and 25 mm under four different input conditions. The results illustrate that loading curves types of the particle velocity significantly influences the stress in brain tissue. The understanding of the influence by the input loading cures can be used to reduce the potentially injury to brain under head impact by designing protective structures to control the loading curves types.

***Keywords*—**Analytical method, mechanical responses, spherical wave propagation, traumatic brain injury.

I. Introduction

TRAUMATIC brain injury (TBI) continues attracting a great deal of attentions due to its irreversible effects and high mortality or disability. Annual head injury statistics show that there are about 1.5 million Americans who suffer TBI each year and 50,000 of them die, 230,000 hospitalize and 80,000-90,000 people experience the onset of long-term disability [1].

On the prevention side, a better understanding of TBI mechanisms is needed. Up to now, much work has been done analytically to investigate the mechanical responses of brain (intracranial pressure, stress and strain). One of the earliest works was done by Anzelius [2], who assumed the head as a rigid spherical vessel fully filled with inviscid fluid. In 1969, Engin [3] proposed an analytical model to study the axisymmetric transient response of a fluid-filled shell subjected to a delta-function impulsive loading, where the shell representing the skull was considered to have membrane and bending properties and the fluid representing the brain was assumed to be inviscid compressible. Based on Engin's model, Talhouni and DiMaggio [4] developed a model considering the skull as a thin elastic prolate spheroidal shell to simulate the head impact by an explosive shock wave. They investigated the distribution of stress in the shell and pressure in the fluid by taking into account eccentricity of the head and found that eccentricity had a significant effect on the brain response. Young [5] proposed a model which combined the Hertzian contact stiffness and the effective bending stiffness of membrane to predict the brain response during head impact. Based on Young's model, Heydari and Jani [6] developed a fluid-filled ellipsoidal shell model with thickness varying, which was more realistic than a spherical model. Up to now, most of these analytical models assumed brain tissue as inviscid fluid whereas the properties of actual brain are more complex According to the experimental and simulative studies, researchers have found that brain tissue behave more like hyper-viscoelastic solid. Therefore, it is worthwhile to further develop hyper-viscoelastic analytical models to study the response of the brain under dynamic loading.

On the other hand, the study of wave propagation in soft tissue has received a great deal of attentions, due to the importance of wave dynamics for the visualization of internal organs or bones. In 1978, Chivers and Parry [7] presented a compilation of acoustic properties (velocity and attenuation) for several mammalian tissues. Kremkau et al. [8] measured wave propagation speed and attenuation in the frequency range of 1 to 5 MHz in 22 tissue samples from six anatomic sites in five normal human brains. Recent studies showed that intracranial wave motion could generate significant intracranial pressure and strain in the brain, especially from the wave produced by the blast loading and high local impact. Thus, it is important to consider the influence of stress wave propagation in the brain when studying the TBI mechanisms. Valdez and Balachandran [9] theoretically investigated wave propagation through brain to understand the influence of nonlinear material properties of the tissues on the propagation characteristics of stress waves generated by transient loading in terms of the propagation speed and attenuation. In their study, the brain was modeled as hyper-viscoelastic solid and wave was assumed to propagate in a one-dimensional rod. All brain fibers are assembled at the center of brain, which cause the stress concentration. This means the maximum stress will always take place at the center of brain, no matter which part of the head is impacted. It is not in accord with the fact that the region of maximum stress and strain is dependent on the impact position.

Y.J. Zhou, is with the School of Mechanical and Aerospace Engineering, Nanyang Technological University, Singapore 639798, Singapore (phone: +65-97970676; e-mail: zhou0191@ e.ntu.edu.sg).

Corresponding Author, G. Lu, is with the School of Mechanical and Aerospace Engineering, Nanyang Technological University, Singapore 639798, Singapore (phone: +65- 6790 5589; e-mail: gxlu@ntu.edu.sg).

It is necessary to develop a reliable method to account for tissue deformation, stress and strain of brain in three-dimensional space. In this study, an analytical method will be used to investigate the wave propagation behavior in a three-dimensional space of a material like human brain tissue under transient loading, where brain tissue is modeled as hyper-viscoelastic solid, which takes into account both nonlinear and time-dependent properties of brain tissue.

II. Analytical Solution for Spherical Wave Propagation

We consider spherical wave propagation within an infinite medium with an initial spherical void. The inner surface is subjected to an initial particle velocity. The responses will be obtained, analytically, in terms of particle velocity and stress as a function of time and position.

A. Governing Equations: Equation of Mass Conservation and Equation of Motion

During the propagation all spherical waves keep the spherical shape with the same center. As shown in Fig. 1, an infinitesimal element is analyzed in the system of spherical coordinates. The strain ε_r and particle velocity v in the radial direction can be expressed as

$$\varepsilon_r(r,t)=\frac{\partial u(r,t)}{\partial r}\ ,v(r,t)=\frac{\partial u(r,t)}{\partial t} \tag{1}$$

where $u(r,t)$ is the radial displacement. Because of spherical symmetry of the motion, the values of circumferential stain in the two principal directions are the same and are determined by

$$\varepsilon_\theta(r,t)=\varepsilon_\varphi(r,t)=\frac{u(r,t)}{r}. \tag{2}$$

Also, $\sigma_\theta(r,t)=\sigma_\varphi(r,t)$. For convenience, we use σ_r , σ_θ , ε_r , ε_θ , and v to represent $\sigma_r(r,t)$, $\sigma_\theta(r,t)$, $\varepsilon_r(r,t)$, $\varepsilon_\theta(r,t)$, and $v(r,t)$, respectively, where σ_r and σ_θ are the radial stress and circumferential stress, respectively.

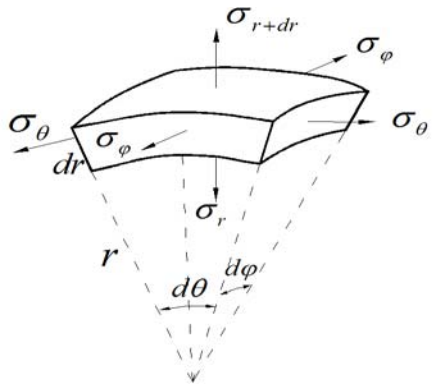

Fig. 1 An infinitesimal element in spherical coordinates (adapted from [11])

The governing equations of spherical waves consist of three parts, the continuity equations, the motion equation and the constitutive equation, which represent the mass conservation, the momentum conservation and material properties, respectively. The continuity equations are given by

$$\frac{\partial\varepsilon_r}{\partial t}-\frac{\partial v}{\partial r}=0 \text{ and } \frac{\partial\varepsilon_\theta}{\partial t}-\frac{v}{r}=0\,, \tag{3}$$

and the equation of motion in the radial direction is expressed as

$$\frac{\partial\sigma_r}{\partial r}+\frac{2(\sigma_r-\sigma_\theta)}{r}-\rho_0\frac{\partial v}{\partial t}=0 \tag{4}$$

where ρ_0 is the density of material. The constitutive equation of material (tissue) is given in the next section.

B. Governing Equations: Constitutive Equation

The material properties are assumed isotropic and homogeneous. The stress in a solid material is based on the changing of volume and shape. To model this nearly incompressible material, brain tissue, the stress is expressed as the sum of a volumetric part, which is determined by volumetric only, and a deviatoric part, which depends on shape change [10]. The volumetric part of the stress is assumed linear elastic, so the bulk modulus, K, is constant. To represent the time-dependent/relaxation effect of brain tissue, the deviatoric part of the stress (shear modules) is modeled visco-elastic, which is formulated in the exponential forms as

$$G(t)=G_\infty+(G_0-G_\infty)e^{-t/\tau}\,, \tag{5}$$

where G_∞, G_0, and τ represent the long-time shear modulus, the short-time shear modulus, and the decay constant, respectively.

To describe the nonlinear part of the model, a hyper-elastic Mooney-Rivlin constitutive law is used. Considering visco-elastic properties, the Mooney-Rivlin constitutive law can be expressed as [12]

$$W=\int_0^t G_1(t-\tau)\frac{\partial}{\partial\tau}(I_1-3)+G_2(t-\tau)\frac{\partial}{\partial\tau}(I_2-3)d\tau\,, \tag{6}$$

where W is the strain energy , I_1 *and* I_2 are strain invariants, $G_{ij}=C_{ij\infty}+C_{ij}e^{-t/\tau_k}$, $k=1$. According to Miller's experimental study [12], it can be assumed that $C_{10\infty}=C_{01\infty}$ and $C_{10}=C_{01}$. Now, using $C_{1\infty}$ and C_1 to represent $C_{01\infty}$ and C_{10} respectively, (6) can be rewritten as

$$\begin{aligned}W&=\int_0^t\left\{\left[C_{1\infty}+C_1e^{-(t-\tau)/\tau_1}\right]\frac{\partial}{\partial\tau}\left[I_1-3+I_2-3\right]\right\}d\tau\\&=\int_0^t\left\{\left[C_{1\infty}+C_1e^{-(t-\tau)/\tau_1}\right]\frac{\partial}{\partial\tau}\left[\lambda^2+2\lambda^{-1}-3+\lambda^{-2}+2\lambda-3\right]\right\}d\tau\end{aligned} \tag{7}$$

The Lagrange stress can be obtained according to the equation $\sigma = \frac{\partial W}{\partial \lambda}$, which gives

$$\sigma = \int_0^t \left[C_{1\infty} + C_1 e^{-(t-\tau)/\tau_1} \right] dN \tag{8}$$

where $N = 2\lambda + 2 - 2\lambda^{-2} - 2\lambda^{-3}$

By using the integration by parts, we can obtain

$$\sigma = N\left[C_{1\infty} + C_1 e^{-(t-\tau)/\tau_1} \right]\Big/_0^t - \frac{1}{\tau_1}\int_0^t \left[C_1 e^{-(t-\tau)/\tau_1} \right] N d\tau \tag{9}$$

or

$$\sigma = CN - N_0\left(C_{1\infty} + C_1 e^{-t/\tau_1}\right) - \frac{1}{\tau_1}\int_0^t \left[C_1 e^{-(t-\tau)/\tau_1} \right] N d\tau \tag{10}$$

where $C = C_{1\infty} + C_1$, $N_0 = (2\lambda + 2 - 2\lambda^{-2} - 2\lambda^{-3})_{t=0}$, or in an equivalent differential form,

$$\frac{\partial \sigma}{\partial t} = C\frac{\partial N}{\partial \lambda}\frac{\partial \lambda}{\partial t} + \frac{C_1}{\tau_1} N_0 e^{-t/\tau_1} - C_1 \frac{1}{\tau_1}\left\{ \left(-\frac{1}{\tau_1} \right) \int_0^t \left[e^{-(t-\tau)/\tau_1} \right] N d\tau + N \right\} \cdot \tag{11}$$

Refer to(10), the integral term can be expressed as

$$-\frac{1}{\tau_1}\int_0^t \left[C_1 e^{-(t-\tau)/\tau_1} \right] N d\tau = \sigma - CN + N_0\left(C_{1\infty} + C_1 e^{-t/\tau_1}\right) \cdot \tag{12}$$

Substituting this into(12), we obtain

$$\frac{\partial \sigma}{\partial t} + \frac{\sigma}{\tau_1} = C\frac{\partial N}{\partial \lambda}\frac{\partial \lambda}{\partial t} + \frac{C_{1\infty}}{\tau_1}\left(N - N_0\right) \tag{13}$$

Between strain and stretch, a relationship is given as $\varepsilon = \frac{1}{2}(\lambda^2 - 1)$ and $\frac{\partial \lambda}{\partial t} = \frac{1}{\sqrt{2\varepsilon + 1}}$, where ε is the Green-Lagrangian strain. Now we can obtain the constitutive relationship of brain tissue in differential form as

$$\frac{\partial \sigma}{\partial t} + \frac{\sigma}{\tau_1} = M\frac{\partial \varepsilon}{\partial t} + \frac{C_{1\infty}}{\tau_1}\left(N - N_0\right) \tag{14}$$

where $M = C\left[2(2\varepsilon + 1)^{-\frac{1}{2}} + 4(2\varepsilon + 1)^{-2} + 6(2\varepsilon + 1)^{-\frac{5}{2}}\right]$.

Similar to the derivation of generalized equation by Wang et al. [11], the three-dimensional nonlinear constitutive equations can be reduced to two parts including the volumetric law and the distortional law due to the spherical symmetry of the motion. The volumetric viscosity can be neglected in wave propagation. Thus, (14) can be expressed as

$$\frac{\partial \sigma_r}{\partial t} + 2\frac{\partial \sigma_\theta}{\partial t} - 3K\left(\frac{\partial \varepsilon_r}{\partial t} + 2\frac{\partial \varepsilon_\theta}{\partial t} \right) = 0 \tag{15}$$

$$\left(\frac{\partial \sigma_r}{\partial t} - \frac{\partial \sigma_\theta}{\partial t} \right) - 2G_{eff}\left(\frac{\partial \varepsilon_r}{\partial t} - \frac{\partial \varepsilon_\theta}{\partial t} \right) + \frac{(\sigma_r - \sigma_\theta) - \left[\sigma_{eff}(\varepsilon_r) - \sigma_{eff}(\varepsilon_\theta) \right]}{\tau_1} = 0, \tag{16}$$

where, $E_{eff} = CM$ is the effective Young's modulus, $G_{eff} = \frac{E_{eff}}{2(1+v)}$ is the effective shear modulus, and $\sigma_{eff}(\varepsilon) = C_{1\infty}(N - N_0)$ is the effective stress.

C. Solution by Characteristic Method

Wang *et al.* [11] proposed the use of characteristic method to analyze the propagation features of spherical waves in engineering plastics. We use the characteristic method to solve the propagation of spherical waves in the brain tissue by transforming those five partial differential equations (two continuity equations, one motion equation, and two constitutive equations) to five ordinary differential equations. The two families of characteristic lines are obtained as follows.

$$\frac{dr}{dt} = \pm\sqrt{\frac{K + \frac{4}{3}G_{eff}}{\rho_0}} = \pm c_k(\varepsilon), \tag{17}$$

where c_k is wave velocity in the brain which is dependent on strain and relaxation time, and $K + \frac{4}{3}G_{eff}$ is defined as wave modulus. The corresponding characteristic compatibility relationship along these two characteristic lines is

$$\begin{aligned} d\sigma_r = {} & \pm\rho_0 c_k dv \mp \frac{2}{3}\frac{\left\{(\sigma_r - \sigma_\theta) - \left[\sigma_{eff}(\varepsilon_r) - \sigma_{eff}(\varepsilon_\theta)\right]\right\}}{c_k \tau_1} dr, \\ & - \frac{2(\sigma_r - \sigma_\theta)}{r} dr \pm \frac{6K - 4G_{eff}}{3c_k}\frac{v}{r} dr \end{aligned} \tag{18}$$

where the plus and minus signs stand for wave propagation direction.

Furthermore, we get the third family of characteristic line

$$dr = 0, \tag{19}$$

and the corresponding characteristic compatibility relationships along this characteristic line are

$$d\sigma_r + 2d\sigma_\theta - 3K\left(d\varepsilon_r + 2d\varepsilon_\theta\right) = 0 \tag{20}$$

$$\left(d\sigma_r - d\sigma_\theta\right) - 2G_{eff}\left(d\varepsilon_r - d\varepsilon_\theta\right) + \frac{\left\{(\sigma_r - \sigma_\theta) - \left[\sigma_{eff}(\varepsilon_r) - \sigma_{eff}(\varepsilon_\theta)\right]\right\}}{\tau_1} dt = 0 \tag{21}$$

$$d\varepsilon_\theta = \frac{v}{r} dt \tag{22}$$

where represents the loci of particle movement, (20) and (21) represent the material constitutive equations along the particle motion locus [11].

III. Numerical Results and Discussion

A numerical solution is conducted to investigate the nonlinear visco-elastic spherical wave propagation in brain tissue by using finite difference method. Based on the previous in this study is given in Table I [13], [14].

TABLE I
MOONEY-RIVLIN AND VISCO-ELASTIC CONSTANTS USED IN THIS STUDY

Tissue	C (Pa)	C_1 (Pa)	$C_{1\infty}$ (Pa)	Bulk modulus K (GPa)	τ_1(s)	Density ρ_0 (kg/m^3)	Poisson's ratio υ
Brain	65	52.5	12.5	2.19	1/125	1040	0.499999

Here, the Mooney-Rivlin constants C is the average of $C10$ and $C01$ used by Kleiven [14]. The C (short-term) to $C_{1\infty}$ (long-term) ratio is taken as 0.19 to derive the values of C_1 and $C_{1\infty}$ [15]. The initial condition is taken as$\sigma_r(r,t) = \sigma_\theta(r,t) = \varepsilon_r(r,t) = \varepsilon_\theta(r,t) = v(r,t) = 0$, and $r_0 \le r \le \infty$ .At r_0, particle velocity as a function of time is applied, corresponding to a sudden internal expansion. The area under this curve represents the total displacement applied atr_0.To evaluate the effect of the loading profile, four loading curves of particle velocity but with the same peak value are applied at $r_0 = 5mm$ (Fig. 2). Fig. 2 (a)-(c) show linearly varying velocity, whereas Fig. 2 (d) represents a nonlinear process which is sine function.

A. Effect of Loading Profile and Peak Value

The mechanical responses at the radii of 5, 6, 10, 15, and 25 mm are obtained. Fig. 3 (a)-(d) show the particle velocity at these radii with corresponding input conditions. As shown in these figures, a common feature exists that with the increasing of wave propagating distance all particle velocity experience attenuation of its amplitude, while the general shape with respect to the peak stress is retained. The attenuation is due to the effect of spherical dispersion and viscous responses induced by the so-called internal dissipative force. Another feature is noted that negative particle velocity appears in Fig. 3 (c) at the end. This is due to the rapid decrease of particle velocity which provides a large inertial resistance to the spherical dispersion.

Fig. 4 (a)-(d) show the radial stress at the different radii under respective input velocity. Similar to particle velocity, the radial stress also attenuates with the propagation of wave in radial direction. The loading profile (a) produces the largest peak compressive radial stress. After the peak, the compressive radial stress reduces to zero and then the stress becomes tensile, due to the decrease of velocity which needs a tensile force to counteract the inertia force. Loading curve (c) causes the largest peak radial tensile stress due to its large acceleration. The occurrence of negative particle velocity in Fig. 3 (c) can be explained by it as well. Note that the values in both peak compressive and tensile stress are very different in Fig. 4 (a)-(d), even though they have the same peak value of input velocity as shown in Fig. 2 (a)-(d). This demonstrates that the loading profile affects the maximum radial stress that the peak values of radial stress are dominated by the rate of change in the input velocity, which is the value of acceleration or deceleration.

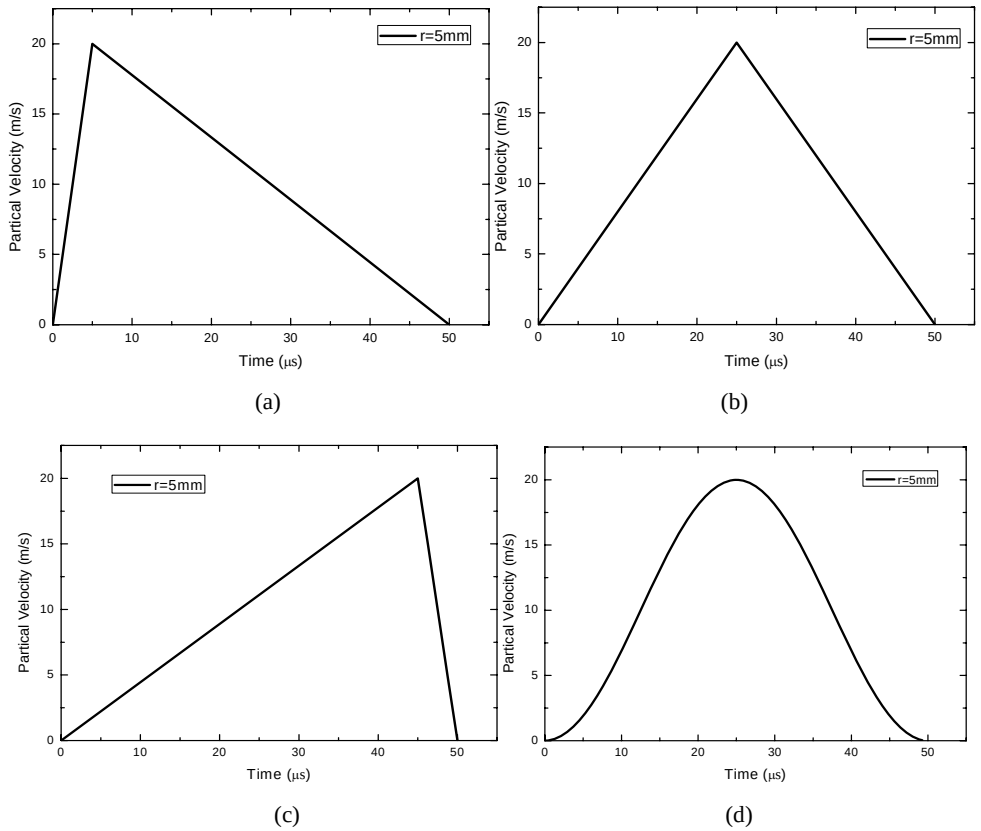

Fig. 2 Input particle velocity time history curves at $r_0 = 5mm$

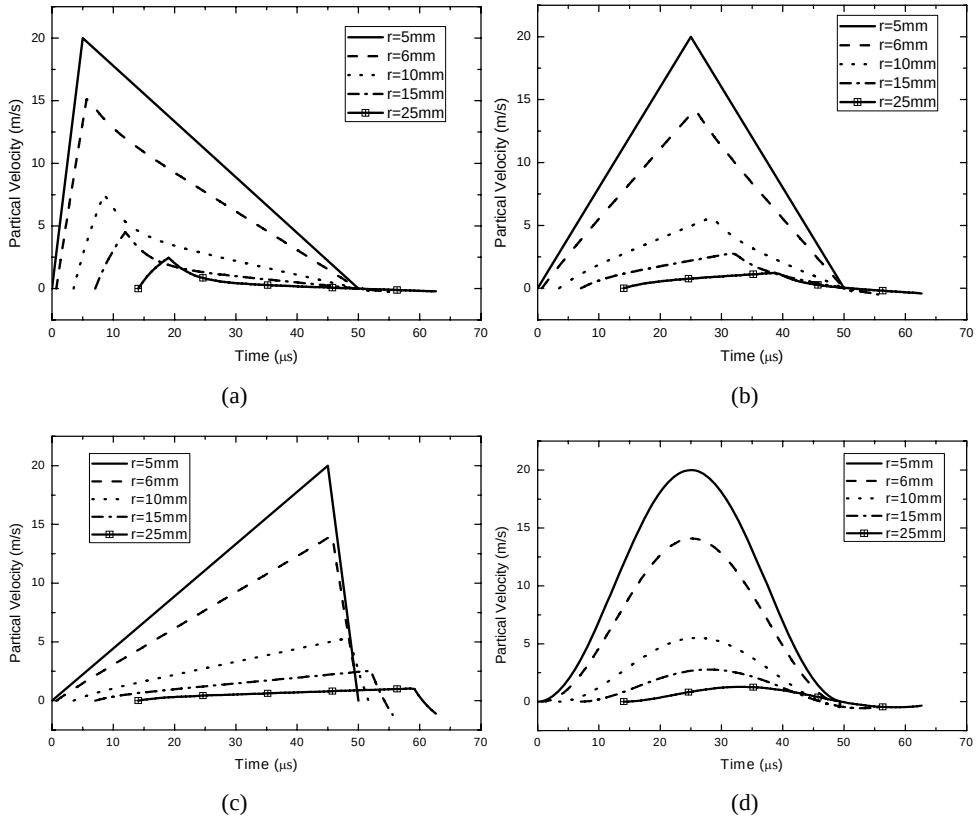

Fig. 3 Particle velocity vs. time curves at r=5, 6, 10, 15, and 25 mm, corresponding to four different inputs in Fig. 2a-d, respectively.

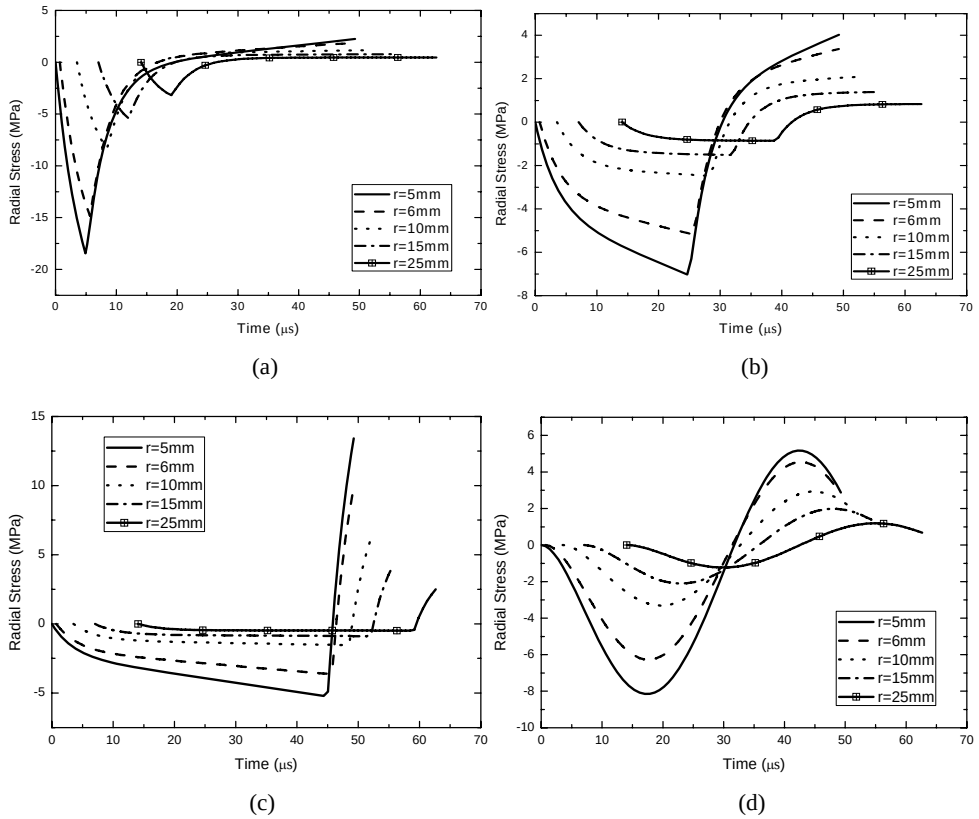

Fig. 4 Radial stress curves at r=5, 6, 10, 15, and 25 mm, corresponding to four different inputs in Figs. 2 (a)-(d), respectively

Fig. 5 (a)-(d) show similar plots to those in Fig. 4 (a)-(d), but for the circumferential stress. The circumferential stress has similar values to those of the radial stress. This is because the effective bulk modulus is of the 10^6 times higher than Young's modulus or shear modulus and the Poisson's ratio used in our numerical study is nearly 0.5 where the brain is approximate to the incompressible material. The compressive circumferential stress takes place when the brain is subjected to sudden internal expansion, whereas it is tensile stress under a static pressure. This may be seen from the motion equation (4). For a static equilibrium equation, the last term of acceleration vanishes. For a compressive radial stress, the circumferential stress is always tensile. However, for a wave problem, when the term for acceleration is sufficiently large, it is possible that a compressive circumferential stress is also obtained, for a compressive radial stress.

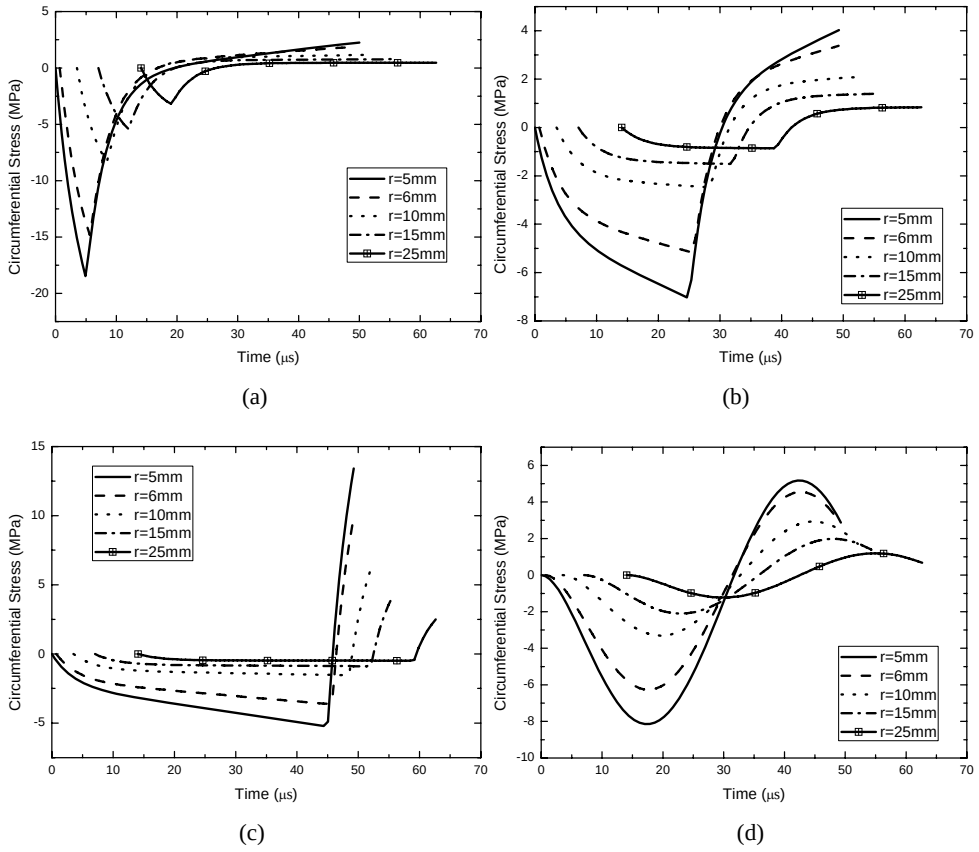

Fig. 5 Circumferential stress curves at r=5, 6, 10, 15, and 25 mm, corresponding to four different inputs in Figs. 2 (a)-(d), respectively.

IV. Conclusions

This paper presents an analytical study of the dynamic behavior of the human brain tissue under sudden internal expansion.

Numerical solution is carried out to investigate the nonlinear visco-elastic spherical wave propagation in the brain tissue by using characteristic method. From the numerical results, following conclusions can be obtained:

1) Particle velocity and stress experience the attenuation with the increasing of propagating distance due to the effect of spherical dispersion and viscous responses.
2) The peak values of radial stress are dominated by the changing rate of input velocity which is the value of acceleration or deceleration. It is possible to reduce the maximum tensile or compressive stress by adjusting the input velocity curve shape without changing the input boundary deformation.
3) The compressive circumferential stress takes place when brain tissue is subjected to sudden internal expansion. This is different from the result of static analysis where it is tensile stress under a static loading. The reason is that the circumferential stress is affected by both inertia force and sudden internal loading.

References

[1] D.J. Thurman, C. Alverson, K.A. Dunn, J. Guerrero, and J.E. Sniezek, "Traumatic brain injury in the United States: A public health perspective," *J. Head. Trauma. Rehab.*, vol. 14, pp. 602-15, 1999.
[2] A. Anzelius, "The effect of an impact on a spherical liquid mass," *Acta. Pathol. Mic. Sc.* , vol. 48, pp. 153-159, 1943.
[3] E. Engin, "Axisymmetric response of a fluid-filled spherical shell to a local radial impulse: a model for head injury," *J. Biomech.*, vol. 2, pp. 325-341, 1969.
[4] O. Talhouni and F. DiMaggio, "Dynamic response of a fluid-filled spheroidal shell—An improved model for studying head injury," *J. Biomech.*, vol. 8, pp. 219-228, 1975.

[5] P.G. Young, "An analytical model to predict the response of fluid-filled shells to impact - a model for blunt head impacts,"*J. Sound. Vib.*, vol. 267, pp. 1107-1126, 2003.
[6] M. Heydari and S. Jani, "An ellipsoidal model for studying response of head impacts,"*Acta. Bioeng. Biomech.*, vol. 12, pp. 47-53, 2010.
[7] R.C. Chivers and R.J. Parry, "Ultrasonic velocity and attenuation in mammalian tissues,"*J. Acoust. Soc. Am.*, vol. 63, pp. 940-953, 1978.
[8] F.W. Kremkau, R.W. Barnes, and C.P. McGraw, "Ultrasonic attenuation and propagation speed in normal human brain,"*J. Acoust. Soc. Am.*, vol. 70, pp. 29-38, 1981.
[9] M. Valdez and B. Balachandran, "Longitudinal nonlinear wave propagation through soft tissue,"*J. Mech. Behav. Biomed. Mater*., vol. 20, pp. 192-208, 2013.
[10] D.W.A. Brands, G.W.M. Peters, and P.H.M. Bovendeerd, "Design and numerical implementation of a 3-D non-linear viscoelastic constitutive model for brain tissue during impact,"*J. Biomech.*, vol. 37, pp. 127-134, 2004.
[11] L.-L. Wang, H.-W. Lai, Z.-J. Wang, and L.-M. Yang, "Studies on nonlinear visco-elastic spherical waves by characteristics analyses and its application,"*Int. J. Impact. Eng.*, vol. 55, pp. 1-10, 2013.
[12] K. Miller and K. Chinzei, "Constitutive modelling of brain tissue: experiment and theory,"*J. Biomech.*, vol. 30, pp. 1115-1121, 1997.
[13] K.K. Mendis, R.L. Stalnaker, and S.H. Advani, "A constitutive relationship for large deformation finite element modeling of brain tissue,"*J. Biomech. Eng.*, vol. 117, pp. 279-85, 1995.
[14] S. Kleiven and W.N. Hardy, "Correlation of an FE model of the human head with local brain motion--consequences for injury prediction,"*Stapp Car Crash J.*, vol. 46, pp. 123-44, 2002.
[15] R.M. Wright, *A computational model for traumatic brain injury based on an axonal injury criterion*. Ann Arbor: The Johns Hopkins University, 2012.